


Experimental Observation of Interorbital Coupling

Diego Guzmán-Silva[✉], Gabriel Cáceres-Aravena, and Rodrigo A. Vicencio

*Departamento de Física and Millenium Institute for Research in Optics-MIRO,
Facultad de Ciencias Físicas y Matemáticas, Universidad de Chile, 8370448 Santiago, Chile*

 (Received 4 March 2021; accepted 15 July 2021; published 6 August 2021)

Interorbital coupling refers to the possibility of exciting orbital states by otherwise orthogonal non-interacting modes, a forbidden process in photonic lattices due to intrinsic propagation constant detuning. In this Letter, using a femtosecond (fs) laser writing technique, we experimentally demonstrate that fundamental and excited orbital states can couple each other when located at different spatial positions. We perform a full characterization of an asymmetric double-well-like potential and implement a scan method to effectively map the dynamics along the propagation coordinate. Our fundamental observation also constitutes a direct solution for a spatial mode converter device, which could be located in any position inside a photonic glass chip. By taking advantage of the phase structure of higher-order photonic modes and the effective negative coupling generated, we propose a trimer configuration as a phase beam splitter, which could be of great relevance for multiplexing and interference-based photonic concatenated operations.

DOI: 10.1103/PhysRevLett.127.066601

The way in which atoms assemble and interact with each other determines their potential to form molecules and matter [1]. These interactions are characterized by different atom states called orbitals. In order to understand and explore otherwise occulted properties, diverse areas of research have proposed the creation of artificial atoms in different physical contexts [2–9]. This includes numerical and experimental research suggesting new materials and the possibility of observing new exotic interactions as solutions for transport and localization of energy, key scientific goals in science. However, although theoretical researchers have assumed the basic and fundamental concept of interorbital interactions as obvious and trivial [10,11], no systematic experimental evidence is found in literature. In this Letter, we demonstrate, both numerically and experimentally, that orthogonal orbital states, located at different 2D photonic atoms, couple each other by an evanescent interaction. We show that symmetric *S*-like wave functions could couple to *P*-like orbitals and also to higher-order states. We use a femtosecond (fs) laser technique [12] to fabricate elliptical 2D waveguides having different propagation constants, which are analogous to different orbital energies. We construct double-well photonic asymmetric potentials [13], such that the on site energies of orthogonal orbitals can be finely tuned and coupling between them becomes possible. Our results offer a new way of studying lattice dynamics where, historically, *S*-like orbitals have mostly been assumed. An interorbital coupling gives the opportunity of tuning the sign of hopping between atoms, increasing the available tools for researchers of different areas and, also, amplifying the possibilities to discover new phenomena [14,15].

The paraxial wave equation in optics and the Schrödinger equation in quantum mechanics have exactly the same mathematical form and, therefore, their mathematical solutions must be equivalent [2]. Theory tells us that a potential-well structure will always have a bound state [1,16], independent of its size (width and depth). However, if we want to excite and observe higher-orbital states, we must satisfy a specific condition that, for one-dimensional structures, reads as

$$8mV_o a^2 \geq h^2 \quad \text{and} \quad 8n_o \Delta n w^2 \geq \lambda^2 \quad (1)$$

for quantum mechanics and optics, respectively. Here m is the particle mass; V_o and a are the potential depth and width, respectively; and h is the Planck constant, while n_o corresponds to the bulk refractive index, Δn is the refractive index contrast, w is the waveguide width, and λ the wavelength. We notice that both relations are equivalent and depend on phenomenologically similar parameters: if the size of atoms or waveguides is larger than some lower bound, higher orbitals are allowed to exist. Specifically in optics, we notice that a larger index contrast and/or a wider waveguide facilitates the generation of a larger number of eigenstates, and waveguides could become multimode depending on the excitation wavelength [16,17].

Resonance is a key concept in physics, and many interactions can be well understood by finding conditions for matching the eigenfrequencies of a given system. Of course, complex resonance problems including different types of interactions [18] are neither trivial nor simple to be described, but the fundamental idea continues to rely on matching or tuning a set of system parameters. Similar to what happens in any physical problem having waves and

restrictions, eigenmodes are classified by their symmetry, where the ground state [10] is always symmetric with respect to the center of the atom or waveguide. This state is the so-called TE00 mode in optics [19] (where TE refers to transverse electric) or ground state in quantum mechanics [1], and has a Gaussian-like profile and larger propagation constant β_S (lower energy). A second state corresponds to a wave function which has a node at the center and, as a consequence, a different phase at different lobes. In optics this state is called TE01 or TE10 depending on its orientation [19], while in atom physics, it is usually called a P state, having also some variations depending on spatial orientation [20]. For simplicity we use the Hydrogen atomlike nomenclature: S and P states for TE00 and TE01/TE10 modes, respectively.

In order to explicitly show interorbital coupling, we follow a simple theoretical idea suggested for cold atom systems [13], as sketched in Fig. 1(a) considering a photonic dimer configuration. Single and multimode waveguides have, in principle, different propagation constants for different orbital states where, for example, $\beta_P < \beta_S$ (in general, propagation constants are always lower for higher-order modes). Therefore, by modifying the local structure of a given waveguide, we can tune its properties and find conditions for an optimal orbital interaction, such that orthogonal states located at different sites have a closer—if not equal—propagation constant. This process would imply an effective dynamical transformation from an S - S interaction into an S - P one, which is the main goal of the present work. We investigate this theoretical concept by, first, numerically integrating a paraxial wave equation considering a coupler (dimer) configuration, which consists of two vertically oriented elliptical waveguides separated by a given distance d [see sketch in Fig. 1(b) and Supplemental Material [21] for details]. We define a relative contrast $\Delta\bar{n} \equiv \Delta n_2 - \Delta n_1$, where Δn_1 and Δn_2 correspond to refractive index contrasts at waveguides 1 and 2, respectively. When both waveguides are equal, a perfect evanescent coupling occurs between S states [2,12,26]. In Fig. 1(b) we show that for $\Delta\bar{n} = 0$ almost 100% of power is effectively transferred to waveguide 2, as expected considering a coupled-mode (discrete) approach [2], which is governed for coupling constant C_S (see Supplemental Material [21]). By increasing the relative contrast $\Delta\bar{n}$, an effective detuning is produced in between the S modes at different waveguides. This diminishes the effective interaction between S states at different positions, and the transferred power is drastically reduced as Fig. 1(b) shows. We observe a minimum transference for a contrast $\Delta\bar{n} \approx 0.25 \times 10^{-3}$. This occurs at the parameter region where the second waveguide starts supporting two modes, as condition (1) suggests. A detuning in propagation constants produces a tendency to localization, due to the creation of a nonsymmetric dimer system with corresponding nonsymmetric eigenstates. On site detuning reduces the

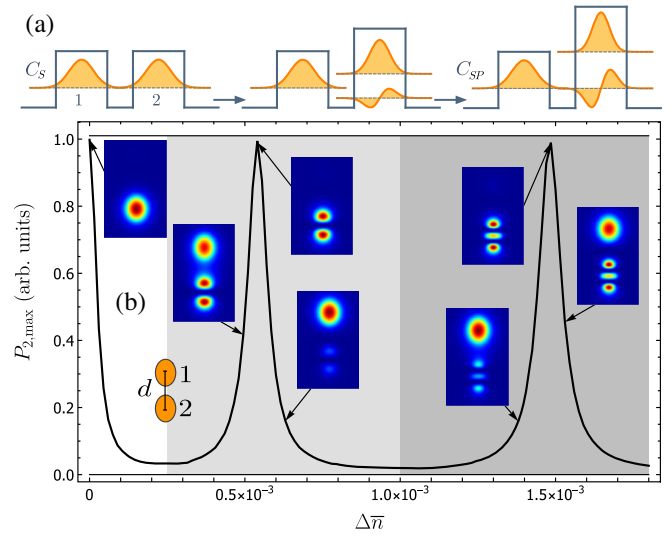


FIG. 1. (a) Propagation constant tuning concept. C_S and C_{SP} correspond to coupling constants in a discrete approach, and define an interaction dynamical scale proportional to $1/C_{S,SP}$. (b) Numerically computed normalized maximum power at waveguide 2 versus refractive index contrast $\Delta\bar{n}$, for two waveguides separated a distance $d = 20 \mu\text{m}$. Insets: numerical intensity profiles at indicated regions. White, light gray, and gray shaded areas indicate one, two, or three modes supported at waveguide 2, respectively. A sketch of a vertically oriented dimer configuration is included.

effective coupling interaction, and the energy tends to remain trapped at the input site. This is phenomenologically similar to a nonlinear dimer [27,28], where the nonlinear response of the system effectively decouples the waveguides due to an effective refractive index change.

By further increasing the refractive index contrast at site 2, in a region where waveguide 2 already supports two modes, we find that the power transfer increases abruptly. We notice that this enhanced transfer is now occurring due to an interaction between the S and P states, as the inset profiles show in Fig. 1(b). This implies that the effective interorbital interaction is switched on, with a coupling constant C_{SP} now governing the dynamics. We find a new peak at $\Delta\bar{n} \approx 0.53 \times 10^{-3}$, where the S power at the first waveguide is almost completely transferred to a P mode at waveguide 2. This sharp peak is an indication that an exact condition for a perfect energy transfer is hard to be achieved numerically and, even more, experimentally (peak at $\Delta\bar{n} = 0$ is sharp, too, but easier to calibrate as both waveguides are equal). Before and after this peak, the transferred energy at site 2 decreases abruptly due to a detuning between the S and P propagation constants, as described in the Supplemental Material [21] for a nonsymmetric dimer model. By further increasing contrast $\Delta\bar{n}$, we observe that the transferred power reduces to a minimum again, this time at $\Delta\bar{n} \approx 1.0 \times 10^{-3}$, in a region where the lower waveguide starts supporting a third state as expected from condition (1). By further increasing

the relative index contrast, we find a new resonant peak at $\Delta\bar{n} \approx 1.5 \times 10^{-3}$. Now, the enhanced transfer of energy at site 2 is due to an interorbital coupling between an S state and a third mode, which we simply call a “Tripole” or “ D ” state (TE₂₀ or TE₀₂ in optics [19]). This mode possesses three lobes and two nodes, with the corresponding phase structure and a vertically oriented profile, due to the waveguide ellipticity. Again, the enhanced peak is quite pronounced, and the condition for perfect conversion is hard to be achieved numerically, and even more so experimentally. So, in principle, this concept could be applied for the excitation—and controlled generation—of any excited state, as soon as the propagation constants at different sites match (see Supplemental Material [21] for more details).

We study optical waveguides as an analogous of 2D photonic atoms by using a fs-laser writing technique [12] (see Supplemental Material [21] for fabrication details). We fabricate several photonic dimer configurations as the examples presented in Fig. 2(a), where bottom waveguides become multimode as the writing power increases (see arrow). In order to characterize the asymmetric dimers, we define the following procedure: (i) single-mode waveguides are fabricated using a fixed writing power $P_1 = 78$ mW along the whole sample (50 mm long) and (ii) we set a writing power (P_2) for waveguide 2 and fabricate eight dimers for this power, having eight different final lengths (Δz) in the interval $\{6, 20\}$ mm, with a step of 2 mm, as sketched in Fig. 2(b). From a discrete model, we expect a cosinelike dynamics along the propagation coordinate, which strongly depends on the coupling constant and effective detuning. As a consequence, the maximum transferred power is obtained at different z values, and the implementation of a z -scan configuration is mandatory in our experiment. We characterize these dimers by focusing a horizontally polarized HeNe laser beam at the input single-mode waveguide, as described in Fig. 2(b). In Fig. 2(c) we show an example of the oscillatory (cosinelike) dynamics for $\Delta P \approx 23$ mW. We clearly observe how light from the S (upper) waveguide starts to, first, weakly excite a P state at the bottom waveguide, while for a larger propagation distance the transferred power increases, with a maximum transference at $\Delta z = 14$ mm. Figure 2(c) directly and quite clearly shows the effective transformation from an S mode into a P state. This observation demonstrates experimentally the theoretical concept described in Fig. 1 and gives strong experimental support for the existence of interorbital coupling in any physical system having orbital-like states. We clearly observe a dynamical oscillation along z as proof of a periodic energy transfer mechanism between neighboring coupled waveguides, which is also strong support for the study of tight-binding (discrete) models including interorbital interactions.

In order to construct a complete parameter space, we analyze several intensity profiles [see the examples shown in the insets of Fig. 2(d)] for 23 different writing powers P_2 .

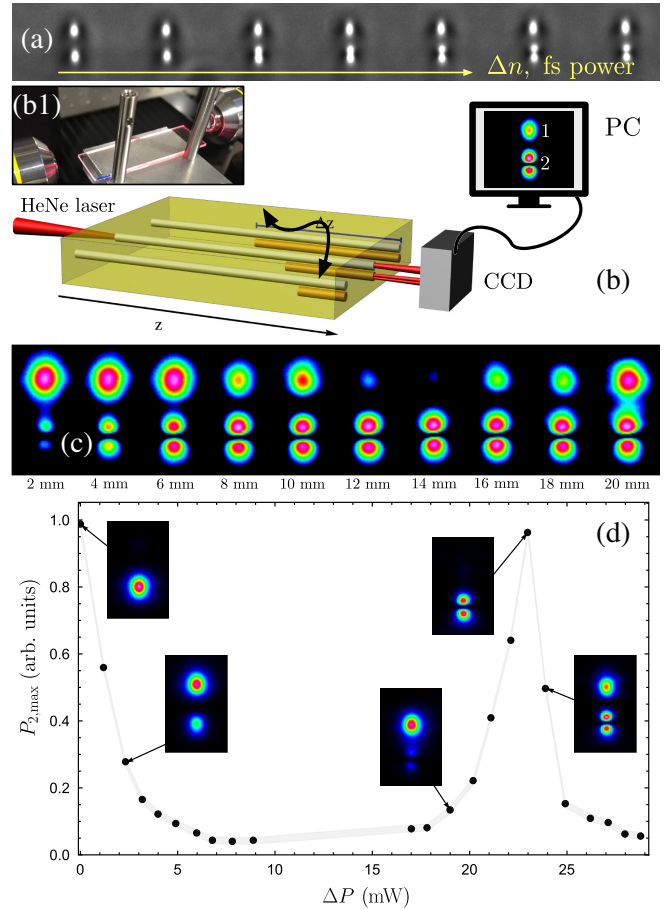


FIG. 2. (a) Microscope image after white light illumination of dimer examples fabricated using a fixed (variable) writing power for upper (bottom) waveguides. (b) Experimental setup for characterizing waveguides and dimers. P (lower, orange) waveguides have a shorter propagation length Δz . (b1) Photograph of the experimental setup. (c) z scan showing interorbital coupling oscillation at different propagation lengths Δz (indicated below each subfigure). (d) Maximum normalized transferred power at waveguide 2 versus fs average laser power difference (ΔP). Every data point was taken at a different distance. Insets: experimental output intensity profiles at parameters indicated by arrows.

Then, we look for the maximum transferred power at waveguide 2, which naturally occurs at different distances [21]. We integrate the intensity at the upper and lower halves of each image and obtain a normalized value. Then, we look for the maximum transference for the eight different propagation lengths, as a result of the z -scan configuration. Figure 2(d) shows our compiled experimental results for maximum transferred power at waveguide 2 versus the fs average laser power difference, which is defined as $\Delta P \equiv P_2 - P_1$. For $\Delta P = 0$, we clearly observe that two identical single-mode waveguides have an excellent transference of energy, with almost 100% of efficiency. Then, by continuing to increase the writing power P_2 , we observe how the transferred power decreases abruptly,

which is in perfect agreement with direct numerical simulations [see Fig. 1(b)], and with a discrete theoretical approach [21].

As our main goal is the observation of interorbital coupling, we continue increasing P_2 and, therefore, $\Delta\bar{n}$ (in our experiment, $\Delta\bar{n} \sim \Delta P$ [21]). For $\Delta P \approx 7$ mW, we observe that the transferred power starts to increase weakly [see Fig. 2(d)]; however, this increment is in the order of the experimental error. We observe a transition region with less than 10% of transfer, for a large ΔP range. However, for $\Delta P \geq 19$ mW we observe a clear increasing tendency and the excitation of a weak P mode at the second waveguide, as a first indication of interorbital interaction. While continuing to increase the writing power P_2 , we observe an abrupt increment of energy at the bottom waveguide, with a clear peak at $\Delta P = 23$ mW, with more than 95% of transference. This peak constitutes concrete experimental proof for the excitation of an orthogonal state at a neighbor waveguide, based on the theoretical concepts described in the previous section. This observation is a result of transforming a given single-mode waveguide into a multimode one, at a given wavelength. We are indeed observing experimentally a propagation constant tuning process, which allows switching on the effective interaction between otherwise noninteracting orthogonal states. The experimental intensity image at peak [inset profile in Fig. 2(d)] shows a perfect generated dipole at the bottom waveguide. This simple observation constitutes two main outcomes of our work: the demonstration of interorbital coupling and a photonic mode converter. The first one is quite a fundamental result: it gives support to different theoretical ideas [10,13,14] coming from diverse research areas [2–9], and it suggests the possibility of studying new lattice configurations considering hybridized interactions [29–33]. Without the demonstrated tuning mechanism, orthogonal states simply do not interact on a lattice, and hybridized physics is simply not possible on a linear regime. The second outcome of our observation is the generation of a simple and concrete method for exciting higher-order spatial states inside a photonic chip, with perfect spatial controllability that can be a key to success for concatenated photonic operations [34–39].

Coupled-mode theory [2] and tight-binding approximation [1] show that modes at different sites (atoms) evanescently interact by a coupling constant C . In Fig. 3(a) we show an experimental characterization of coupling coefficients for different separation distances and for different orbital states [see examples of SP dimers at the inset of Fig. 3(a) and [21] for more details]. We observe a clear exponentially decaying tendency [12] for all coupling coefficients. As the profiles in Fig. 2(c) show, the S mode wave function, although being broad, is very well trapped at the waveguide region, while the P mode, in general, occupies a larger vertical area. Therefore, we expect that $|C_S| < |C_{SP}| < |C_P|$, as our experimental data show in

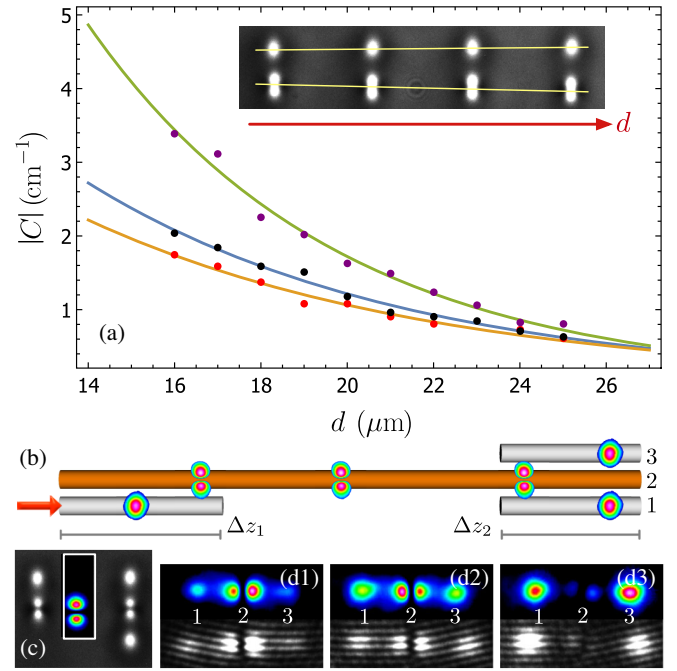


FIG. 3. (a) Absolute coupling constant $|C|$ versus distance for S - S (red dots), S - P (black dots), and P - P (purple dots) interactions, with lines representing exponential fits. Inset: a white light microscope image for S - P dimers having different separation distances d . (b) SP dimer + SPS trimer configuration to demonstrate a phase beam splitter. (c) White light microscope image for an SP dimer and an SPS trimer. Inset: the output profile for the SP dimer only. (d1)–(d3) Output images, for $\Delta z_2 = 2, 4, 6$ mm, respectively, after laser excitation of an S waveguide at the input facet. Top and bottom images correspond to intensity and phase profiles, respectively.

Fig. 3(a) for any distance d (in general, $C_S > 0$ and $C_P < 0$, while the C_{SP} sign depends on orbital orientation [15,17,32,33]). This is the first time that this tendency and dependence are clearly and directly shown experimentally for S and P states, giving strong support for theoretical studies considering different and more complex spatial configurations. It is worth mentioning that the tendency shown in Fig. 3(a) strongly depends on waveguide orientation, which in our case is vertical [see the inset of Fig. 1(b)].

As an application of the interorbital coupling, we experimentally show the different phases induced due to hybridized interactions. As it has been suggested theoretically [13,33], an interorbital interaction produces the appearance of negative coupling constants, which could be of great impact to the study of topology and effective magnetic fields on lattices [15,40]. Therefore, our method looks to be a promising and simple way of generating synthetic magnetic fields [41] on lattices, which could have an important impact when considering topological properties [42] as well. In order to show experimental evidence for this effect, we fabricate a setup consisting of an SP dimer

plus an SPS-trimer configuration, as sketched in Fig. 3(b). We focus a HeNe laser beam at the single-mode (white) waveguide and generate a perfect P state at the multimode (orange) waveguide, after a coupling distance of $\Delta z_1 = 14$ mm [Fig. 3(c), left, shows an SP dimer]. Afterward, the P state propagates freely along the z direction for about 30 mm. Then it acts as an input excitation for an SPS-trimer configuration [see Fig. 3(c), right] and interacts symmetrically with both neighboring single-mode waveguides. As expected, interorbital coupling occurs again, and new S modes are generated back in waveguides 1 and 3, as shown in Fig. 3(d), top. Interestingly, by taking advantage of the phase structure of the P state we are able to induce a π phase shift in between the two generated S states. Figure 3(d), bottom, shows different interferograms (see Supplemental Material [21] for details) with a clear π phase shift in between the right and left parts of the output profiles. This clearly indicates that the coupling interaction to the right and to the left single-mode waveguides are effectively opposite in sign, which is direct proof for a negative coupling constant [15]. This system is also an example for a phase π beam splitter, which could be quite useful for interferometric quantum optics [38,43,44], considering concatenated operations [34]. The output profile also coincides with the flatband mode of a rhombic lattice [45], which is an important subject of research nowadays in photonic lattices.

In conclusion, we have demonstrated numerically and experimentally an interorbital coupling interaction between S and P states on a photonic platform. We first corroborated a resonance picture by numerically integrating a paraxial wave equation and clearly observed the coupling between different orbitals, as a consequence of asymmetrizing a double-well-like potential photonic structure [13]. This process was implemented with high precision using a fs-laser writing technique, allowing the excitation of higher-order states and experimentally probing negative coupling interactions. Our method also offers a new technique for exciting higher-order spatial states inside an optical chip, which could have a great impact on multiplexing applications [46,47]. The possibility of locating the mode conversion system in any arbitrary position is a direct advantage compared with lithographic-like techniques [43,48–52]. Our observation constitutes a fundamental validation of interorbital coupling, which could be an important new ingredient for further studies in lattice science, but, also, a key tool for concatenated or multiplexing photonic operations in the classical and quantum regimes.

The authors acknowledge stimulating discussions with Magnus Johansson, Luis Foa, and Bastian Real. This Letter was supported in part by Millennium Science Initiative Program ICN17-012 and FONDECYT Grants No. 1191205 and No. 3190601.

- [1] E. Kaxiras, *Atomic and Electronic Structure of Solids* (Cambridge University Press, Cambridge, England, 2003).
- [2] D. N. Christodoulides, F. Lederer, and Y. Silberberg, *Nature (London)* **424**, 817 (2003).
- [3] I. Bloch, *Nat. Phys.* **1**, 23 (2005).
- [4] P. St-Jean, V. Goblot, E. Galopin, A. Lemaître, T. Ozawa, L. Le Gratiet, I. Sagnes, J. Bloch, and A. Amo, *Nat. Photonics* **11**, 651 (2017).
- [5] S. H. Mousavi, A. B. Khanikaev, and Z. Wang, *Nat. Commun.* **6**, 8682 (2015).
- [6] M. Brandenbourger, X. Locsin, E. Lerner, and C. Coullais, *Nat. Commun.* **10**, 4608 (2019).
- [7] M. Sato, B. E. Hubbard, and A. J. Sievers, *Rev. Mod. Phys.* **78**, 137 (2006).
- [8] V. D. Pham, K. Kanisawa, and S. Fölsch, *Phys. Rev. Lett.* **123**, 066801 (2019).
- [9] Y. Wang, P. Surendran, S. Jose, T. Tran, I. Herrera, S. Whitlock, R. McLean, A. Sidorov, and P. Hannaford, *Sci. Bull.* **61**, 1097 (2016).
- [10] X. Li and W. V. Liu, *Rep. Prog. Phys.* **79**, 116401 (2016).
- [11] F. Mangussi, I. Sagnes, A. Harouri, A. Lemaître, J. Bloch, A. Amo, and G. Usaj, *J. Phys: Condens. Matter* **32**, 315402 (2020).
- [12] A. Szameit, D. Blömer, J. Burghoff, T. Schreiber, T. Pertsch, S. Nolte, A. Tünnermann, and F. Lederer, *Opt. Express* **13**, 10552 (2005).
- [13] X. Li, E. Zhao, and W. V. Liu, *Nat. Commun.* **4**, 1523 (2013).
- [14] S. Sil, S. N. Karmakar, and R. K. Moitra, *Phys. Lett. A* **183**, 344 (1993).
- [15] M. Kremer, I. Petrides, E. Meyer, M. Heinrich, O. Zilberberg, and A. Szameit, *Nat. Commun.* **11**, 907 (2020).
- [16] A. W. Snyder and J. D. Love, *Optical Waveguide Theory* (Chapman & Hall, New York, 1983).
- [17] C. Cantillano, L. Morales-Inostroza, B. Real, S. Rojas-Rojas, A. Delgado, A. Szameit, and R. A. Vicencio, *Sci. Bull.* **62**, 339 (2017).
- [18] G. A. Jones and D. S. Bradshaw, *Front. Phys.* **7**, 100 (2019).
- [19] A. Lipson, S. G. Lipson, and H. Lipson, *Optical Physics* (Cambridge University Press, Cambridge, England, 2010).
- [20] M. Ölschläger, T. Kock, G. Wirth, A. Ewerbeck, C. Morais Smith, and A. Hemmerich, *New J. Phys.* **15**, 083041 (2013).
- [21] See Supplemental Material at <http://link.aps.org/supplemental/10.1103/PhysRevLett.127.066601> for more details, which includes Refs. [22–25].
- [22] K. Kawano and T. Kitoh, *Introduction to Optical Waveguide Analysis: Solving Maxwells Equation and the Schrödinger Equation* (Wiley & Sons, New York, 2001).
- [23] G. L. Pedrola, *Beam Propagation Method for Design of Optical Waveguide Devices* (Wiley & Sons, New York, 2015).
- [24] Y. Nasu, M. Kohtoku, and Y. Hibino, *Opt. Lett.* **30**, 723 (2005).
- [25] Y. Plotnik, M. C. Rechtsman, D. Song, M. Heinrich, J. M. Zeuner, S. Nolte, Y. Lumer, N. Malkova, J. Xu, A. Szameit, Z. Chen, and M. Segev, *Nat. Mater.* **13**, 57 (2014).
- [26] C. Cantillano, S. Mukherjee, L. Morales-Inostroza, B. Real, G. Cáceres-Aravena, C. Hermann-Avigliano, R. R. Thomson, and R. A. Vicencio, *New J. Phys.* **20**, 033028 (2018).
- [27] S. M. Jensen, *IEEE J. Quantum Electron.* **18**, 1580 (1982).

- [28] M. Albiez, R. Gati, J. Fölling, S. Hunsmann, M. Cristiani, and M. K. Oberthaler, *Phys. Rev. Lett.* **95**, 010402 (2005).
- [29] M. Johansson, A. A. Sukhorukov, and Y. S. Kivshar, *Phys. Rev. E* **80**, 046604 (2009).
- [30] C. Wu, D. Bergman, L. Balents, and S. Das Sarma, *Phys. Rev. Lett.* **99**, 070401 (2007).
- [31] S. Yin, J. E. Baarsma, M. O. J. Heikkinen, J.-P. Martikainen, and P. Törmä, *Phys. Rev. A* **92**, 053616 (2015).
- [32] G. Cáceres-Aravena and R. A. Vicencio, *Phys. Rev. A* **100**, 013803 (2019).
- [33] G. Cáceres-Aravena, L. E. F. Foa Torres, and R. A. Vicencio, *Phys. Rev. A* **102**, 023505 (2020).
- [34] A. Peruzzo, M. Lobino, J. C. F. Matthews, N. Matsuda, A. Politi, K. Poulios, X.-Q. Zhou, Y. Lahini, N. Ismail, K. Wörhoff, Y. Bromberg, Y. Silberberg, M. G. Thompson, and J. L. O'Brien, *Science* **329**, 1500 (2010).
- [35] R. Keil, M. Heinrich, F. Dreisow, T. Pertsch, A. Tünnermann, S. Nolte, D. N. Christodoulides, and A. Szameit, *Sci. Rep.* **1**, 94 (2011).
- [36] G. Masada, K. Miyata, A. Politi, T. Hashimoto, J. L. O'Brien, and A. Furusawa, *Nat. Photonics* **9**, 316 (2015).
- [37] B. Real, C. Cantillano, D. López-González, A. Szameit, M. Aono, M. Naruse, S.-J. Kim, K. Wang, and R. A. Vicencio, *Sci. Rep.* **7**, 15085 (2017).
- [38] D. W. Canning, R. J. Donaldson, S. Mukherjee, R. J. Collins, L. Mazzarella, U. Zanforlin, J. Jeffers, R. R. Thomson, and G. S. Buller, *Opt. Express* **27**, 31713 (2019).
- [39] S. Slussarenko and G. J. Pryde, *Appl. Phys. Rev.* **6**, 041303 (2019).
- [40] S. Mukherjee, M. Di Liberto, P. Öhberg, R. R. Thomson, and N. Goldman, *Phys. Rev. Lett.* **121**, 075502 (2018).
- [41] P. Wang, L. Chen, C. Mi, Z. Meng, L. Huang, K. Sadiq Nawaz, H. Cai, D.-W. Wang, S.-Y. Zhu, and J. Zhang, *npj Quantum Inf.* **6**, 18 (2020).
- [42] T. Ozawa, H. M. Price, A. Amo, N. Goldman, M. Hafezi, L. Lu, M. C. Rechtsman, D. Schuster, J. Simon, O. Zilberberg, and I. Carusotto, *Rev. Mod. Phys.* **91**, 015006 (2019).
- [43] A. Mohanty, M. Zhang, A. Dutt, S. Ramelow, P. Nussenzveig, and M. Lipson, *Nat. Commun.* **8**, 14010 (2017).
- [44] J.-L. Tambasco, G. Corrielli, R. J. Chapman, A. Crespi, O. Zilberberg, R. Osellame, and A. Peruzzo, *Sci. Adv.* **4**, eaat3187 (2018).
- [45] S. Mukherjee and R. R. Thomson, *Opt. Lett.* **40**, 5443 (2015).
- [46] R. G. H. Van Uden, R. Amezcua Correa, E. Antonio Lopez, F. M. Huijskens, C. Xia, G. Li, A. Schülzgen, H. de Waardt, A. M. J. Koonen, and C. M. Okonkwo, *Nat. Photonics* **8**, 865 (2014).
- [47] T. Mizuno and Y. Miyamoto, *Opt. Fiber Technol.* **35**, 108 (2017).
- [48] Z. Li, M.-H. Kim, C. Wang, Z. Han, S. Shrestha, A. C. Overvig, M. Lu, A. Stein, A. M. Agarwal, M. Lončar, and N. Yu, *Nat. Nanotechnol.* **12**, 675 (2017).
- [49] Y. Greenberg and A. Karabchevsky, *Appl. Opt.* **58**, F21 (2019).
- [50] Y. Li, F. Liu, Y. Huang, B. Fan, and R. Wan, *Opt. Commun.* **289**, 60 (2013).
- [51] Y. Ding, F. Da Ros, B. Huang, H. Ou, and C. Peucheret, *Opt. Express* **21**, 10376 (2013).
- [52] S. Zheng, M. Huang, X. Cao, L. Wang, Z. Ruan, L. Shen, and J. Wang, *Photonics Res.* **7**, 1030 (2019).